acta physica slovaca vol. 55 No. 5, 429 – 434 **October 2005**

INVESTIGATION OF ATMOSPHERIC PRESSURE PLASMA-JET SYSTEM USED FOR DEPOSITION OF ZnO THIN FILMS[1]

M. Chichina[2]† ‡, O. Churpita ‡ , Z. Hubička ‡ , M. Tichý† ,
M. Holdová ‡, P. Virostko † ‡
† *Charles University in Prague, Faculty of Mathematics and Physics, Department of Electronics and Vacuum Physics, V Holešovičkách 2, 180 00 Prague, Czech Republic*
‡ *Institute of Physics, Division of Optics, Academy of Sciences of the Czech Republic, Na Slovance 2, 18221 Prague 8, Czech Republic*

Received 18 April 2005, in final form 1 July 2005, accepted 8 July 2005

We report on the barrier-multi-torch plasma-jet system — the novel plasma deposition system capable of working at atmospheric pressure in open air. This system can be operated in continuous-wave mode as well as in pulse regime. In the paper we describe time evolution of light intensity during single impulse in the multi-torch plasma jet system recorded by digital cine camera. Plasma jet impedance in the active part of the impulse was determined by direct voltage and current measurements using digital phosphor oscilloscope.

PACS: 52.75.Kq, 52.77.Fv, 52.80.Pj

1 Introduction

The atmospheric plasma deposition of various thin films is subject of great interest. A large number of systems for atmospheric PECVD (Plasma Enhanced Chemical Vapor Deposition) have been developed recently [1]. Low temperature dielectric-barrier discharges are very often applied for PECVD of polymer and other kinds of thin films [2]. The atmospheric RF barrier-torch plasma jet described in [3] was already applied for the low temperature deposition of In_xO_y and SnO_x thin films on polymer substrates [4, 5].

2 Experiment

In its simplest configuration, the barrier-torch discharge is generated inside the thin quartz glass pipe near the sharp edge of the metallic RF electrode, which is placed outside the quartz glass tube (see schematic diagram in Fig. 1 and photo in Fig. 2). Several such RF electrodes with pipes can be configured in line. This multi plasma-jet system (photo in Fig. 3) treats wider

[1] Presented at Joint 15th Symposium on Applications of Plasma Processes (SAPP) and 3rd EU-Japan Symposium on Plasma Processing, Podbanské (Slovakia), 15 – 20 January 2005.

[2] E-mail address: chichina@mbox.troja.mff.cuni.cz

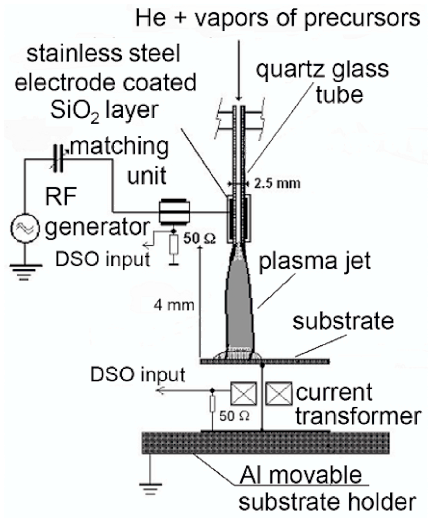

Fig. 1. The barrier-torch atmospheric-pressure plasma-jet system used for deposition of ZnO thin films.

substrate area at once and hence relatively large substrate surface can be processed by simple linear movement of the substrate holder [3]. In comparison with the single plasma jet system the multi-jet needs, apart from the main RF electrode, a supplementary, auxiliary RF electrode, which is also depicted in Fig. 3. This electrode helps to ignite the discharge and prevents the discharge from burning in the upstream direction. Our experience shows that combination of the main and auxiliary electrodes results in proper driving the discharge towards the dielectric substrate. Auxiliary electrode is connected with the main RF electrode via 737 Ω resistor. Glass pipes and the main RF electrode are cooled down by the (closed circuit) flow of distilled water.

The RF electrode is connected with the RF power generator with a frequency 13.56 MHz via the matching unit. The RF power was modulated with a square pulse from pulse generator with the repetition period of 50 ms. The length t_a of the active part of the cycle was 5 ms (duty cycle 1:9). The absorbed power in the discharge in the burning phase of the cycle was 37 W. This modulation allowed formation of high density plasma in the active part of the duty cycle and simultaneously kept the neutral gas in the plasma jets at the substrate sufficiently cold thus protecting polymer substrate from thermal damages.

Helium gas was used and fed into the system of four quartz nozzles. In the process of ZnO films deposition vapours of Zn-acetylacetonate ($Zn(C_5H_7O_2)_2$) were used as precursors of layer material (ZnO) and mixed with the helium carrier gas prior to entering the RF excitation area. The precursor flow rate could not be measured. It was expected that by accurately keeping the precursor container temperature the rate of sublimation remained constant and hence also the precursor flow rate. The given precursor temperature of 70 °C has been determined empirically. Bare polymer (kapton) foil, silicon and quartz glass were used as substrates. Coating of the larger substrate area was provided by motor-driven x-y movement of the substrate.

RF wattmeters were used for measurement of the applied and reflected RF power at the out-

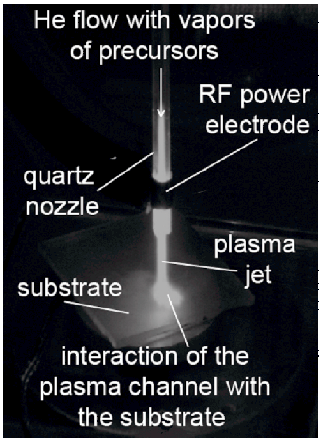

Fig. 2. Photo of single barrier-torch discharge.

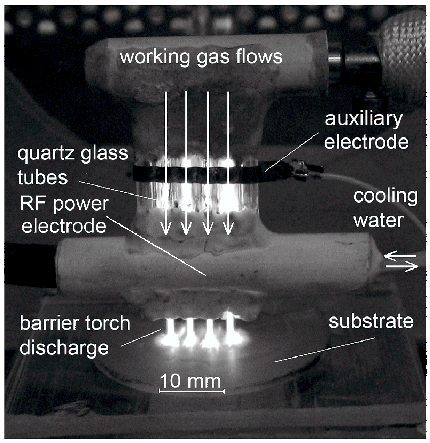

Fig. 3. Photo of multi barrier-torch discharge.

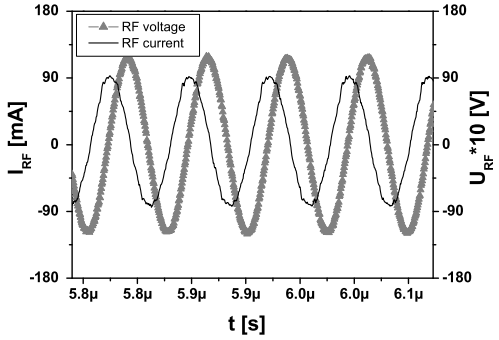

Fig. 4. Time dependences of RF voltage and RF current recorded on barrier-torch discharge in helium using digital oscilloscope.

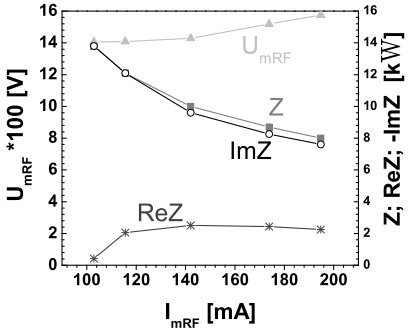

Fig. 5. Real and imaginary parts and modulus of the discharge impedance and RF voltage amplitude vs RF current amplitude.

put of the RF generator. However, the power obtained as a difference of the readings of those watmetters can be far from the real absorbed power in the discharge channel. Comparatively large part of the generator power is namely wasted in the matching network due to high recirculating currents. For example, with low-pressure RF glow discharges the RF power losses in the matching unit amounted to 10%–90% of the generator power (of the difference between the applied and reflected power) depending on discharge conditions. In order to avoid the mentioned problem, we determined the power absorbed in the presented discharge system by direct phase-sensitive measurement of the RF discharge voltage and current. The discharge voltage was measured using high-voltage oscilloscope probe and the discharge current was sensed using

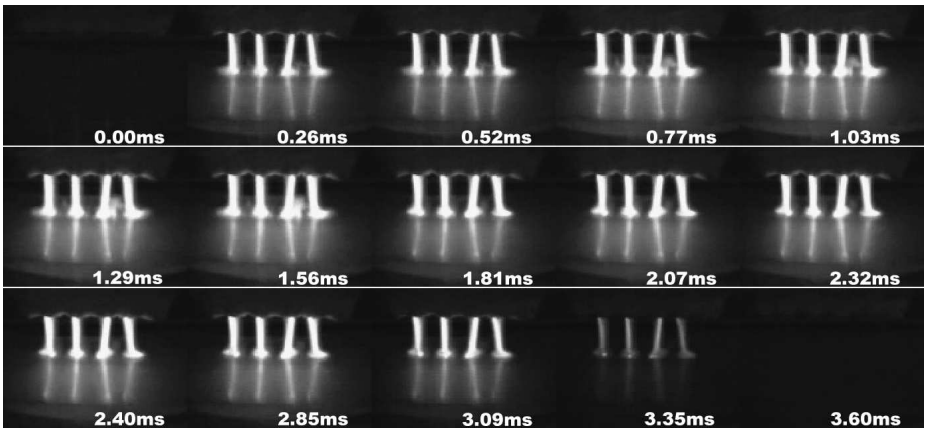

Fig. 6. Time evolution of barrier-torch discharge. Time is counted from the beginning of the RF impulse.

the Rogowski coil. In this manner it was possible to display on the oscilloscope screen directly the waveforms of the discharge voltage and current U_{RF} and I_{RF}, from which it was easy to read out the respective amplitudes and the phase shift ϕ. Using those values it was possible to calculate the real and imaginary parts of total discharge impedance Z according to the formulas:

$$\mathrm{Re}Z = (U_{RFm}/I_{RFm})\cos(|\phi|), \qquad \mathrm{Im}Z = -(U_{RFm}/I_{RFm})\sin(|\phi|) \tag{1}$$

U_{RFm} and I_{RFm} represent the respective amplitude of RF voltage/current. In Fig. 4 we depicted the RF voltage and current waveforms measured directly on the discharge during the active part of modulation cycle. The real and imaginary parts of the plasma column impedance calculated according to formulas (1) are displayed in Fig. 5 in dependence on the amplitude of the RF current together with the modulus of the impedance and amplitude of the RF voltage. In accordance with the expectations the imaginary part of the plasma impedance decreases with increasing the RF current while the real part at low RF currents rises and then stays more or less independent of the RF current. The absolute value of the impedance hence decreases with increasing RF current and the peak RF voltage slowly rises with RF current. In our measurements we did not detect significant dependence of the RF current on the flow rate of working gas.

ZnO films deposited on silicon were analyzed by electron microprobe. The analysis has shown that the films had chemical composition very close to stoichiometric ZnO. The described regime of the multi-torch plasma-jet system enabled also deposition of ZnO films on polymer surface without the need to change any of the external process parameters (peak power, duty cycle, repetition frequency). Electrical conductivity of ZnO films deposited on kapton was measured by four-points van der Pauw method [6].

3 Results

We performed deposition of ZnO thin films onto silicon and polymer (kapton) substrates. The regular deposition time amounted to approximately 15–30 minutes. The corresponding film

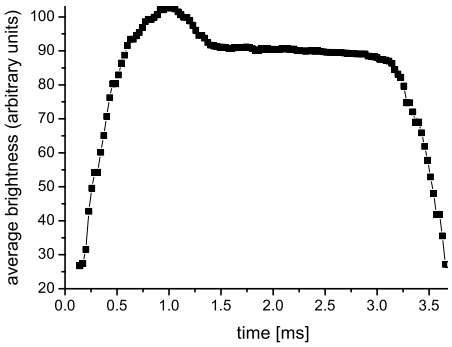

Fig. 7. Time evolution of the discharge brightness during active impulse.

thickness was around 300 nm depending on the applied power (duty cycle) and deposition time. The ZnO layers deposited on polymer contained hexagonal crystalline phase; they were optically transparent and had electrical conductivity $\sigma = 10^{-1}$–10^{0} S/cm. ZnO films with such parameters find important applications, e.g. in display engineering and in solar cell technology.

To help understanding the nature of the barrier torch discharge during the active period of the cycle we recorded the light intensity of the discharge using the digital video camera Panasonic NV-DS65EG.

We observed the whole visible range and no filters were used. If the repetition frequency of the discharge was adjusted close to the frame frequency the video camera yielded stroboscopic effect. The video camera frame rate was 30 frames per second (30 Hz). In this case we adjusted the discharge repetition frequency to 29.975 Hz. Because of the difference between frame rate f_1 and the discharge repetition frequency f_2 every frame taken by the camera is shifted by the delay $\tau = 1/f_1 - 1/f_2$ with respect to the start of the discharge impulse. For given frequencies this delay amounts to approximately 28 μs. It means that we can obtain approximately t_a/τ frames during the active part of the discharge period. In this manner we could obtain time evolution of the light intensity from the discharge during the active impulse with good time resolution.

In Fig. 6 we see 15 frames recorded over the discharge active period and some time after switch-off. In these measurements the duration of the discharge impulse was 3 ms, time length of the record depicted in Fig. 6 was 3.6 ms. The discharge impulse repetition frequency was in this case 29.79 Hz. The background in the recorded frames was very dark and hence we could assume that the vast majority of bright pixels in each digital frame record were produced by light emitted by burning discharge.

Based on that assumption we calculated the average brightness of each frame using standard routine in Adobe Photoshop 8.0 software. In this manner it was possible to construct evolution of the light intensity of the discharge over the whole active period, i.e. the ignition of the discharge, its development during the burning period and its decay (extinction) after switching off the RF power, see Fig. 7. The discharge impulse length was again 3 ms, the discharge repetition frequency was in this case 29.975 Hz. This corresponded to 125 video frames over the record period 3.6 ms. From this figure we can assess rise time of the light intensity after switch-on of the RF power (approximately 0.5 ms) and its fall time after the RF power has been switched off

(approximately 0.4 ms). The rise and fall time of the RF power impulse was in the order of 20 μs i.e. much less than rise and fall times of the light intensity. Interesting feature of the dependence in Fig. 7 is the local maximum of the light intensity at the beginning of the active impulse. This is most probably connected with the fact that at the beginning of the power impulse the plasma is being created and hence the matching between the generator and plasma is not perfect. RF generator yields in this period of time larger voltage since its load impedance is far form optimum. RF voltage on the powered electrode exhibits therefore maximum at the beginning of the impulse. This effect was checked by recording the peak RF voltage using the digital processing oscilloscope. After the plasma is ignited matching abruptly improves (matching unit is adjusted to minimum reflected power during the active discharge phase) and larger power is absorbed in plasma. This results in greater light intensity at the beginning of the active discharge impulse. The comparatively long plasma decay after RF power has been switched off can be explained by slower diffusion at atmospheric pressure and by the effect of long-lived Helium metastables $He(2^3S_1)$ and $He(2^1S_0)$ with lifetimes 6×10^{-5} s and 2×10^{-2} s respectively.

4 Discussion

Deposition rate, ZnO layer adhesion and quality were strongly dependent on measured electric parameters of plasma-jet, on repetition frequency and on duty cycle. The quality of the layer, deposition rate and adhesion has improved at higher magnitudes of RF voltage and RF current in the plasma jet channel. On the other hand increasing of these parameters was limited by overheating of the substrate, especially in case of plastic substrates.

The method of video filming with a stroboscopic effect has shown a considerable promise for mobile diagnostic of the plasma. This method seems to be very easy to setup and understand, it is fast and relatively cheap. The reproducibility of discharge impulse was good; this is demonstrated by "sleek" curve in Fig. 7, which was taken during 125 different impulses without large experimental data dispersion.

Acknowledgement: This work was supported by Grant Agency of the AS CR, grant S1010203, by Czech Science Foundation, grants 202/03/H162, 202/03/0827 and 202/04/0360 and by project COST action 527. This work is a part of the research plan MSM 0021620834 that is financed by the Ministry of Education of the Czech Republic.

References

[1] A. M. Nardes, A. M. De Andrade, F. J. Fonseca, E. A. T. Dirani, E. A. T. Dirani, R. Muccillo, E. N. S. Muccillo : *Journal of materials science-materials in electronics* **14(5-7)** (2003) 407

[2] K. G. Donohoe, T. Wydeven: *J. Appl. Polymer Sci.* **23** (1979) 2591

[3] Z. Hubicka, M. Cada,M Sicha, A. Churpita, P. Pokorny, L. Soukup, L. Jastrabik: *Plasma Sources Science & Technol.* **11** (2002) 195

[4] M. Cada, O. Churpita, Z. Hubicka, H. Sichova, L. Jastrabik: *Surf. Coat. Tech.* **177** (2004) 699

[5] O. Churpita, Z. Hubicka, M. Cada, D. Chvostova, L. Soukup, L. Jastrabik, P. Ptacek: *Surf. Coat. Tech.* **174** (2003) 1059

[6] L. J. van der Pauw: *Philips Tech. Rev* **20** (1958) 220